

Chemical composition of evolved stars in the young open clusters NGC 4609 and NGC 5316 [★]

Arnas Drazdauskas,¹† Gražina Tautvaišienė,¹ Rodolfo Smiljanic,²
Vilius Bagdonas,¹ and Yuriy Chorniy¹

¹*Institute of Theoretical Physics and Astronomy, Vilnius University, Saulėtekio al. 10222 Vilnius, Lithuania*

²*Nicolaus Copernicus Astronomical Center, Polish Academy of Sciences, Bartycka 18, 00-716, Warsaw, Poland*

Accepted 2016 July 12. Received 2016 July 1

ABSTRACT

High-resolution spectral analysis is performed for the first time in evolved stars of two young open clusters: NGC 4609 and NGC 5316, of about 80 and 100 Myr in age, respectively, and turn-off masses above 5 M_{\odot} . Stellar evolution models predict an extra-mixing event in evolved stars, which follows the first dredge-up and happens later on the red giant branch. However, it is still not understood how this process affects stars of different masses. In this study, we determine abundances of the mixing sensitive elements carbon and nitrogen, carbon isotope $^{12}\text{C}/^{13}\text{C}$ ratios, as well as 20 other elements produced by different nucleosynthetic processes (O, Na, Mg, Al, Si, Ca, Sc, Ti, Cr, Mn, Co, Ni, Y, Zr, Ba, La, Ce, Pr, Nd, and Eu). We compared our results with the latest theoretical models of evolutionary mixing processes. We find that the obtained $^{12}\text{C}/^{13}\text{C}$ and C/N ratios and [Na/Fe] agree quite well with the model which takes into account thermohaline- and rotation-induced mixing but within error limits also agree with the standard first dredge-up model. Comparison of oxygen, magnesium and other α -elements with theoretical models of Galactic chemical evolution revealed that both clusters follow the thin disk α -element trends. Neutron-capture element abundances in NGC 4609 are apparently reflecting its birthplace in the thin disk, while NGC 5316 has marginally higher abundances, which would indicate its birthplace in an environment more enriched with neutron-capture elements.

Key words: Galaxy: abundances – Galaxy: evolution – stars: abundances – stars: evolution – open clusters and associations: individual: NGC 4609 – open clusters and associations: individual: NGC 5316

1 INTRODUCTION

We continue investigations of evolutionary mixing processes in evolved stars of open clusters (OCs; Mikolaitis et al. 2012; Tautvaišienė et al. 2015; Drazdauskas et al. 2016 and references therein). The study of stars in OCs gives us many advantages when compared to a single object analysis. With a sample of stars of roughly the same origin (age, distance, metallicity), we can greatly improve the accuracy of the analysis. OCs span a variety of ages, distances and positions in the Galaxy. They have stars in different stages of evolution, which is beneficial when trying to understand evo-

lutionary effects on the changes of the photospheric chemical composition.

Analysing the chemical composition of stars can provide not only insights into stellar evolution, but into the evolution of the Galaxy as well. OCs with multiple objects can provide us with better determinations of their positions in the Galaxy (distance from the Sun and the centre of the Galaxy) and their ages than we can derive for single stars. Having multiple stars in a single OC can provide better statistics for determination of chemical abundances. Combining the more precise positions, with accurate chemical element abundance determinations gives us an opportunity to study abundance gradients in our Galaxy. Among the most important galactic evolution indicators are the α -elements. According to numerous studies, there is a significant difference between α -element abundances in different parts of the Galaxy (Bensby et al. 2014; Neves et al. 2009 and references therein). In addition to light chemical

[★] Based on observations collected at the European Organisation for Astronomical Research in the Southern Hemisphere under ESO programme 085.D-0093(A).

† E-mail: arnas.drazdauskas@tfai.vu.lt

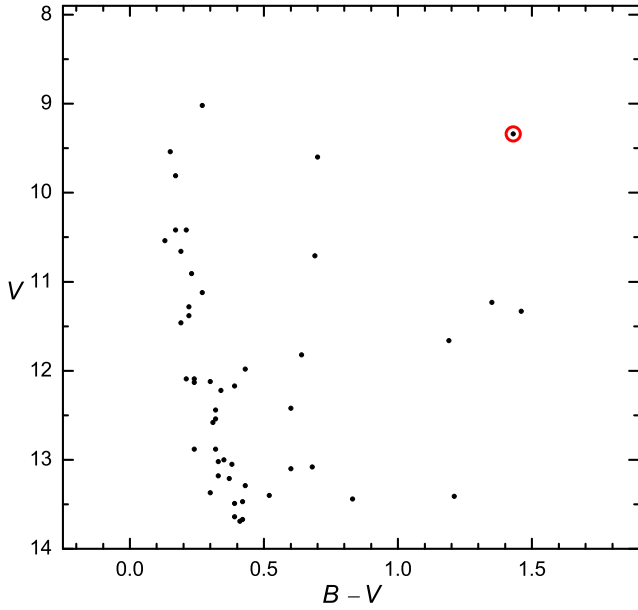


Figure 1. The colour-magnitude diagram of the open cluster NGC 4609. The star investigated in this work is indicated by the open circle. The diagram is based on *UBV* photometry by [Feinstein & Marraco \(1971\)](#)

elements, we determine heavy element abundances as well. The so called s- and r-process elements are produced during neutron capture processes ([Burbidge et al. 1957](#)) at different stages of stellar evolution. It is well known that asymptotic giant branch (AGB) stars are mainly responsible for synthesis of s-process elements. However, their influence on production of these elements was underestimated, especially in young clusters ([D’Orazi et al. 2009](#); [Jacobson & Friel 2013](#)). The site of the r-process nucleosynthesis is still under debate, possibilities include core collapse supernovae (e.g., [Woosley et al. 1994](#); [Nishimura et al. 2015](#)) and neutron star mergers ([Eichler et al. 1989](#); [Freiburghaus et al. 1999](#)). Comparing the neutron capture element abundances with the metallicity, we can gain valuable insights into the evolution of our Galaxy ([Maiorca et al. 2011, 2012](#); [Reddy et al. 2012, 2013, 2015](#); [Mishenina et al. 2015](#); [Overbeek et al. 2016](#)).

Our main goal is to determine abundances of mixing sensitive chemical elements, and carbon and nitrogen in particular. Through CNO cycle, CNO elements play an important role as energy sources in stellar interiors. This affects stellar positions in a Hertzsprung-Russel (HR) diagram and the production of heavy chemical elements. The carbon and nitrogen abundances, C/N, and carbon isotope ratios $^{12}\text{C}/^{13}\text{C}$ are important tools to study stellar evolution. When low- and intermediate-mass stars are at the bottom of the giant branch, the first dredge-up takes place ([Iben 1965](#)). Surface abundances are further modified when extra-mixing processes become efficient. This happens when low-mass stars reach the luminosity bump on the red giant branch (RGB). Variations of $^{12}\text{C}/^{13}\text{C}$ and C/N ratios depend on several factors: stellar evolutionary stage, mass, and metallicity ([Gilroy 1989](#); [Luck 1994](#); [Gratton et al. 2000](#); [Tautvaišienė et al. 2000](#); [Tautvaišienė et al. 2005, 2010](#); [Smiljanic et al. 2009, 2016](#); [Mikolaitis et al. 2010](#),

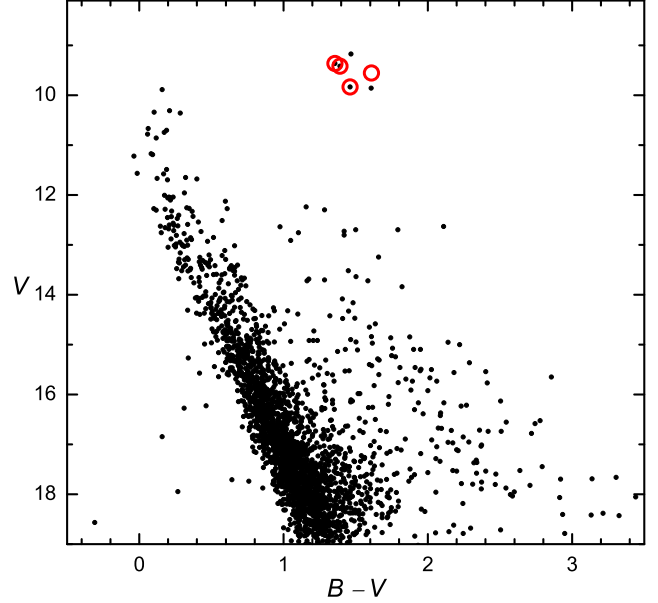


Figure 2. The colour-magnitude diagram of the open cluster NGC 5316. The stars investigated in this work are indicated by open circles. The diagram and the three stars are based on *UBV* CCD photometry by [Carraro & Seleznev \(2012\)](#) and the star marked by empty circle is from T. Oja (private communication)

[2011a,b, 2012](#)). On the other hand, exact dependencies are still uncertain ([Chanamé et al. 2005](#); [Charbonnel 2006](#); [Cantiello & Langer 2010](#); [Charbonnel & Lagarde 2010](#); [Denissenkov 2010](#); [Lagarde et al. 2011, 2012](#); [Wachlin et al. 2011](#); [Angelou et al. 2012](#); [Lattanzio et al. 2015](#)). There are models which predict different outcomes of mixing effects depending on the stellar turn-off (TO) mass. In this work, we try to fill a lack of observational data in the TO mass range $>5 M_{\odot}$ by analysing two relatively young open clusters.

The first-targeted cluster in our work is NGC 4609. There are only a few previous photometric studies and no spectroscopic ones for this cluster. The first ever study of NGC 4609 was by [Feinstein & Marraco \(1971\)](#). Their photoelectric *UBV* observations and analysis of the cluster provided an age of 60 Myr and a distance of 1320 pc as well as identified 33 true members. Consecutive age determinations range from 36 Myr ([Battinelli & Capuzzo-Dolcetta 1991](#)) to 125 Myr ([Kharchenko et al. 2013](#)). The following photometric study by [Mermilliod \(1981\)](#) confirmed that the distance is about 1325 pc, and provided values for the reddening $E(B - V) = 0.34$ and extinction $(m - M) = 11.68$. [Jura \(1987\)](#) made a rough estimate of TO mass to be around $7 M_{\odot}$. The only metallicity determination was made by [Claria et al. \(1989a\)](#). They obtained *UBV*, David Dunlap Observatory (DDO) and Washington photometry for G and K stars and found a metallicity of about 0.05 ± 0.13 .

The second open cluster analysed in this work is NGC 5316. The first photometric age and distance determination was made by [Lindoff \(1968\)](#). They derived an age of 51 Myr and a distance around 1.12 kpc. The following photometric analysis of the cluster provided similar distance values, ranging from 1.08 kpc ([Becker & Fenkart 1971](#)) to 2 kpc ([Chen et al. 2003](#)). The determined Galactocentric distances do not vary much as well (from 7.4 kpc by [Chen et al.](#)

2003 to 7.84 kpc by Strobel 1991). Age determinations however vary more significantly from the already mentioned determination by Lindoff (1968) to around 195 Myr determined by Battinelli & Capuzzo-Dolcetta (1991). The most recent determination of about 170 Myr comes from Kharchenko et al. (2013). The newest most comprehensive study by Carraro & Seleznev (2012) from *UBVI* CCD photometry provided an age of 100 Myr, a distance of 1.4 kpc and R_{gc} of 7.6 kpc, as well as values for reddening $E(B-V) = 0.25 \pm 0.05$ and extinction $(m-M) = 11.50 \pm 0.2$. The only TO mass determination was made by Jura (1987), who provides a value of about $4 M_{\odot}$.

NGC 5316 has numerous photometric metallicity determinations. The first one being by Claria et al. (1989a) who used multiple photometric systems to derive $[Fe/H] = 0.19 \pm 0.11$ from seven RGB stars. The following studies by Piatti et al. (1995) and Twarog et al. (1997) used the same *DDO* photometry as Claria et al. (1989a), however different analysis methods were applied. The resulting derived abundances were $[Fe/H] = -0.02 \pm 0.12$ and $[Fe/H] = 0.13 \pm 0.13$, respectively. The newest study by Kharchenko et al. (2013) provides the metallicity of $[Fe/H] = 0.05 \pm 0.13$ based on two stars.

2 OBSERVATIONS

The observations were carried out using bench-mounted, high-resolution, astronomical Échelle spectrograph FEROS (Fiber-fed Extended Range Optical Spectrograph; Kaufer et al. 1999) at the 2.2 m Max Planck Gesellschaft/European Southern Observatory (ESO) Telescope in La Silla, between 2010 June 25 and 27. FEROS provides a full wavelength coverage of 3500–9200 Å over 39 orders with a resolving power of about 48000. All spectra were reduced with the FEROS DRS (Data Reduction System) pipeline within MIDAS.

A total of 5 stars were observed (one in NGC 4609 and four in NGC 5316). As can be seen in Figs. 1 and 2, the chosen stars are at the position of the red clump. We present parameters of the observed stars and a log of observations in Table 1. The magnitudes were taken from the same sources as for the CMD diagrams (see Figs. 1 and 2). The heliocentric radial velocities were computed in this work using DAOSPEC (Stetson & Pancino 2008) with the Gaia-ESO line list (Heiter et al. 2015) and the IRAF task RVCORRECT. Radial velocity values from the WEBDA database Mermilliod et al. (2008) are listed as well and are in agreement with our results.

2.1 Membership

NGC 4609 is a poorly populated cluster with only one red giant in its field (NGC 4609 43 or HD 110478). A comprehensive radial velocity membership study has never been performed for this cluster. The radial velocity monitoring of the star 43 by Mermilliod et al. (2008) suggests that this is a single star. The proper motion analysis of many open clusters by Dias et al. (2014) includes stars in NGC 4609, but does not include the star 43. Only photometric membership analyses have been performed. The first photometric study of this cluster remains as its most comprehensive photometric

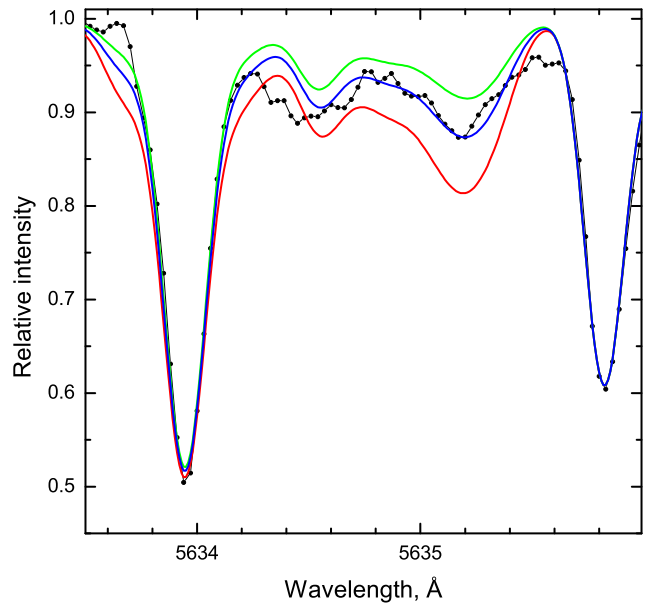


Figure 3. A fit to the C_2 Swan (0,1) band head at 5635.5 Å in the star NGC 5316 45. The observed spectrum is shown as a black line with dots. The synthetic spectra with $[C/Fe] = -0.08 \pm 0.1$ are shown as solid lines.

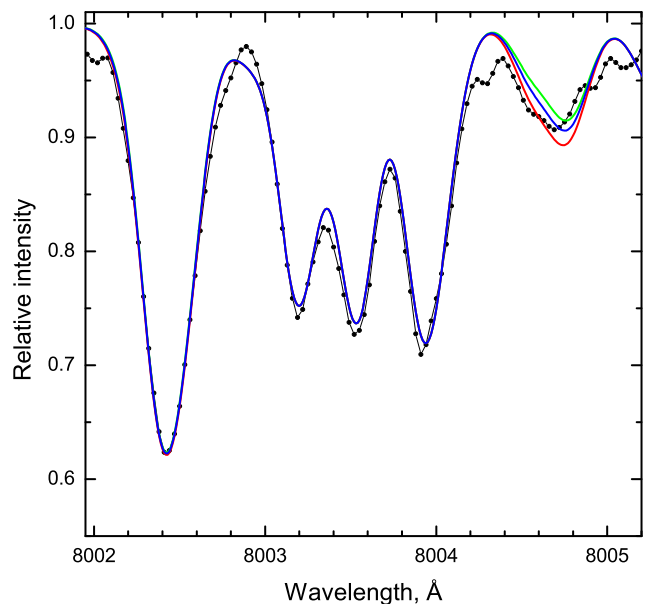


Figure 4. A fit to the CN bands in the star NGC 4609 43. The observed spectrum is shown as a black line with dots. The synthetic spectra with $^{12}C/^{13}C$ ratio 23 ± 5 are shown as solid lines.

study (Feinstein & Marraco 1971). In that paper, photometry was obtained for 52 stars out of which 33 are considered to be members (including the red giant), although the membership criteria are not explained. Claria et al. (1989b) further obtained and analyzed *UBV*, *DDO*, and Washington photometry of this giant and concluded that it is a cluster member based on two criteria. The first compares the reddening computed for the red giant with that obtained for the main-sequence stars. The second compares the predicted luminosity class of the giant, given the cluster distance, with

Table 1. Parameters of the programme stars and a log of observations

ID	<i>V</i> mag	<i>B</i> – <i>V</i> mag	$RV_{\text{This work}}$ km s ⁻¹	σ km s ⁻¹	RV_{WEBDA} km s ⁻¹	R.A. deg (J2000)	DEC deg (J2000)	Time obs.	Exp. time seconds	S/N
NGC 4609										
43	9.34	1.43	-20.74	0.56	-21.30	301.9865	-00.0553	2010-06-23	600	~180
NGC 5316										
31	9.39	1.43	-13.50	0.75	-14.71	310.1919	+00.1544	2010-06-25	600	~200
35	9.44	1.48	-15.03	0.60	-15.53	310.1819	+00.1307	2010-06-25	600	~200
45	9.55	1.61	-13.79	0.66	-14.45	310.2426	+00.1333	2010-06-27	600	~200
72	9.84	1.59	-15.52	0.70	-15.72	310.2247	+00.1239	2010-06-27	900	~150

that derived using DDO indices. According to [Claria et al. \(1989a\)](#), the results of both methods indicate that the star 43 is a member of NGC 4609.

The photometric studies by [Rahim \(1966\)](#) and [Carraro & Seleznev \(2012\)](#), both down to $V \sim 16$, find up to seven candidate red giants in the field of NGC 5316. The four stars from NGC 5316 that are analyzed in this work were originally chosen from the radial velocity study of [Mermilliod et al. \(2008\)](#). These authors monitored six red giants in the field of the cluster. The four stars (NGC 5316 31, 35, 45, and 72) were found to be members, while the remaining two are non-members and spectroscopic binaries. The analysis of Tycho 2 proper motions by [Dias et al. \(2002\)](#) found that the stars NGC 31, 35, 45, and 72 have membership probabilities of 83%, 76%, 78%, and 86%, respectively. Moreover, we note that [Claria & Lapasset \(1989\)](#) analyzed *UBV*, DDO, and Washington photometry of seven giants in the field of NGC 5316. These authors applied the same two membership methods discussed above for NGC 4609, and found that only the four stars analyzed in our work are confirmed members of NGC 5316.

3 METHOD OF ANALYSIS

Atmospheric parameters of stars were determined using the standard spectroscopic method. The effective temperature (T_{eff}) was determined requiring that the abundance of Fe I lines did not depend on the lower level excitation potential (χ). The surface gravities ($\log g$) were determined from the iron ionization equilibrium. The microturbulence velocity (v_t) was found by minimising a scatter between abundances of Fe I lines and assuming that there should be no relation between abundances and equivalent widths. Determining these three main parameters through multiple iterations provides us with the value of metallicity as calculated from the used Fe I lines. We used between 22 and 29 Fe I lines to derive the atmospheric parameters and metallicity content for the target stars.

We analysed the spectra using a differential analysis technique. All calculations were differential with respect to the Sun. Solar element abundance values were taken from [Grevesse & Sauval \(2002\)](#). For the abundance calculations which were based on equivalent widths of spectral lines we used the EQWIDTH code, and for those which were based on spectral synthesis we used the BSYN code, both developed at the Uppsala Observatory. A set of plane-parallel, one-dimensional, hydrostatic, constant flux LTE model at-

mospheres were taken from the MARCS stellar model atmosphere and flux library¹ described by [Gustafsson et al. \(2008\)](#).

We used equivalent widths for the determination of abundances for Na, Mg, Al, Si, Ca, Sc, Ti, Cr, Mn, Co, and Ni chemical elements. Each line for these elements was inspected and some of them were excluded due to blending or other contamination effects, hence the line list differs slightly for every star. For this task we used the SPLAT-VO ([Škoda et al. 2014](#)) tool developed by the German Astrophysical Virtual Observatory and the Astronomical Institute of the Academy of Sciences of the Czech Republic. For abundance calculations for the mentioned elements we used neutral lines, however we determined the Ti II abundance from ionized lines as well.

Spectral synthesis was used for C, N, O, and neutron-capture chemical element abundance determinations as well as for ¹²C/¹³C ratio calculations. The Vienna Atomic Line Data Base (VALD, [Piskunov et al. 1995](#)) was used to prepare input data for the calculations and the atomic oscillator strengths for the lines used were taken from the inverse solar spectrum analysis by [Gurtovenko & Kostyk \(1989\)](#).

For the carbon abundance determination in all stars we used two regions: C₂ Swan (0,1) band heads at 5135.5 Å and 5635.2 Å. We used the same molecular data of C₂ as by [Gonzalez et al. \(1998\)](#). The oxygen abundance was derived from synthesis of the forbidden [O I] line at 6300 Å. The *gf* values for ⁵⁸Ni and ⁶⁰Ni isotopic line components, which blend the oxygen line, were taken from [Johansson et al. \(2003\)](#). An interval of 7980-8010 Å containing strong CN features was used to determine nitrogen abundance and ¹²C/¹³C ratios. The ¹²C/¹³C ratio was obtained from the ¹³C/¹²N feature at 8004.7 Å. The CN molecular data for this wavelength interval were provided by Bertrand Plez. Figs. 3 and 4 display examples of spectrum syntheses for the programme stars. The best-fitting abundances were determined by eye.

The sodium abundance was determined from three or four lines (4751.8, 5682.6, 6154.2 and 6160.8 Å). We applied non-local thermodynamic equilibrium (NLTE) corrections as described in the paper by [Lind et al. \(2011\)](#). The corrections range from -0.09 dex in the star NGC 5316 35 to -0.12 dex in NGC 5316 31 and NGC 5316 72. The magnesium abundance was determined from equivalent widths of two or three Mg I lines (5711.09, 6318.70, and 6319.24 Å).

Abundances for neutron-capture chemical elements in

¹ <http://marcs.astro.uu.se/>

Table 2. Effects on derived abundances, $\Delta[A/H]$, resulting from model changes for the star NGC 4609 43.

Species	ΔT_{eff} ± 100 K	$\Delta \log g$ ± 0.5	Δv_t ± 0.3 km s $^{-1}$	$\Delta[\text{Fe}/\text{H}]$ ± 0.1	Total
C (C ₂)	0.01	0.08	0.00	0.02	0.08
N (CN)	0.05	0.07	0.01	0.02	0.09
O ([O I])	0.01	0.13	0.00	0.03	0.13
¹² C/ ¹³ C	1	1	0	0	1.4
Na I (LTE)	0.09	0.04	0.10	0.03	0.14
Mg I	0.02	0.02	0.04	0.01	0.05
Al I	0.08	0.01	0.07	0.02	0.10
Si I	0.05	0.07	0.08	0.01	0.11
Ca I	0.11	0.01	0.13	0.02	0.16
Sc I	0.02	0.13	0.11	0.04	0.17
Ti I	0.14	0.01	0.13	0.02	0.19
Ti II	0.02	0.13	0.13	0.04	0.19
Cr I	0.10	0.01	0.15	0.02	0.18
Mn I	0.09	0.06	0.16	0.03	0.19
Co I	0.04	0.06	0.15	0.02	0.17
Ni I	0.01	0.06	0.16	0.11	0.17
Y II	0.01	0.13	0.07	0.04	0.15
Zr I	0.20	0.02	0.06	0.01	0.21
Ba II	0.05	0.14	0.45	0.04	0.47
La II	0.02	0.14	0.01	0.03	0.14
Ce II	0.02	0.13	0.08	0.05	0.15
Pr II	0.03	0.13	0.00	0.05	0.14
Nd II	0.03	0.13	0.19	0.04	0.23
Eu II	0.01	0.14	0.01	0.04	0.14

our programme stars were derived using synthetic spectra. We used ionized lines for elements Y, Ba, La, Ce, Pr, Nd, Eu and neutral - for Zr. Y was determined from the Y II lines at 4883.69, 4900.12, 4982.14, 5200.41, 5402.78 Å; Zr from the Zr I lines at 5385.1 and 6127.5 Å; Ba from the Ba II lines at 6141.00 and 6496.91 Å; La from the La II lines at 4748.73, 6320.41, 6369.48 Å; Ce from the Ce II lines at 4773.96, 5274.22, 5512.00, 5610.3, 6043.00 Å; and Nd abundance was derived from the Nd II lines at 5092.8, 5255.52, 5293.2, 5319.8 Å. After careful line inspection, we have chosen between one and five lines for each element. Every spectral line fit was inspected individually and after such inspection some of the lines were excluded due to their apparent asymmetry or particularly high deviation of abundance from remaining lines for that element.

A hyperfine structure (HFS) was taken into account for the synthesis of barium line at 6496.9 Å (McWilliam 1998) as well as for the Pr II lines at 5259.7 and 5322.8 Å (Snedden et al. 2009). The europium abundance was determined from a single Eu II feature at 6645.1 Å. The wavelength, excitation energy and total $\log gf = 0.12$ were taken from Lawler et al. (2001), the isotopic fractions of ¹⁵¹Eu 47.77% and ¹⁵³Eu 52.23%, and isotopic shifts were taken from Biehl (1976). We also took into account the partial blending of the said line with Si I and Ca I lines at 6645.21 Å.

Since stellar rotation can be important when analysing young stars, we estimated it by looking at stronger surrounding lines in spectral regions around the investigated C, N, and O features. Our roughly estimated values are presented together with the atmospheric parameters in Sect. 4.

Two types of uncertainties should be taken into account.

First, we have the errors that affect each line independently: uncertainties of atomic parameters, placement of the local continuum, and the fitting of the line itself. Secondly, there are errors that affect all lines at the same time (such as uncertainties in the stellar atmospheric parameters and the model used).

Table 2 shows a relation between the abundance estimates $[\text{E}/\text{Fe}]$ and assumed uncertainties of the atmospheric parameters in the programme star NGC 4609 43. Considering the given deviations from the used parameters, we see that the abundances of the majority of chemical elements are not affected strongly. However, Ba II lines are very sensitive to the microturbulence velocity for a set of atmospheric parameters of this star.

A scatter of the deduced line abundances gives an estimate of the uncertainty due to the random errors. The uncertainties in the derived abundances that are the result of random errors amount to approximately 0.06 dex.

Since abundances of C, N, and O are also bound together by the molecular equilibrium in the stellar atmospheres, we further investigated how an error in one of them typically affects the abundance determination of another. Thus $\Delta[\text{O}/\text{H}] = 0.10$ causes $\Delta[\text{C}/\text{H}] = 0.04$ and $\Delta[\text{N}/\text{H}] = 0.08$; $\Delta[\text{C}/\text{H}] = 0.10$ causes $\Delta[\text{N}/\text{H}] = -0.10$ and $\Delta[\text{O}/\text{H}] = 0.02$; $\Delta[\text{N}/\text{H}] = 0.10$ has no effect on either the carbon or the oxygen abundances.

4 RESULTS AND DISCUSSION

4.1 Parameters of open clusters

The determined atmospheric parameters for the target stars are presented in Table 3. We determined a metallicity of $[\text{Fe}/\text{H}] = 0.16 \pm 0.08$ for NGC 4609 which is slightly larger than the only previous photometric determination by Claria et al. (1989a) who found $[\text{Fe}/\text{H}] = 0.05 \pm 0.13$. As it was mentioned before, NGC 5316 also had only photometric metallicity determinations ranging from $[\text{Fe}/\text{H}] = 0.19$ to $[\text{Fe}/\text{H}] = -0.02$, and our result of $[\text{Fe}/\text{H}] = -0.02 \pm 0.05$ agrees quite well with those studies.

The newly determined metallicities of the clusters and the ages from literature were used to compute the PARSEC isochrones (Bressan et al. 2012) and to determine the TO masses for the target clusters. We derived a TO mass of $\sim 5.6 M_{\odot}$ with the adopted age of 80 Myr (determined by Kharchenko et al. 2005) for NGC 4609, and $\sim 5 M_{\odot}$ with the age of 100 Myr (determined by Carraro & Seleznev 2012) for NGC 5316.

We also have calculated a rough estimate of the Galactocentric distance for NGC 4609, as no value could be found in previous studies. We took the galactic coordinates, the distance from the Sun derived by Kharchenko et al. (2013) ($d = 1.3$ kpc), and the Galactocentric distance of 7.98 kpc for the Sun as determined by Zhu & Shen (2013) from Galactic Cepheids. Our result for the Galactocentric distance of NGC 4609 is ~ 7.5 kpc. We also redetermined the galactocentric distance of NGC 5316 using the distance value from Kharchenko et al. (2013), and we get $R_{\text{gc}} = \sim 7.4$ kpc for NGC 5316. Our recalculated value is very close to the most recent estimate of 7.6 kpc by Carraro & Seleznev (2012), although they used slightly larger distance values for their determination ($d_{\odot} = 1.4$ kpc and $R_{\text{gc}\odot} = 8.5$ kpc).

Table 3. Main atmospheric parameters of programme stars

ID	T_{eff} K	$\log g$	v_t km s ⁻¹	$v \sin i$ km s ⁻¹	[Fe/H]	σ_{FeI}	n	σ_{FeII}	n
NGC 4609									
43	4620	2.20	1.45	2.0	0.16	0.08	29	0.03	6
NGC 5316									
31	4825	1.70	1.85	6.9	0.05	0.05	28	0.04	4
35	4650	2.00	2.05	5.2	-0.03	0.07	29	0.02	4
45	4500	1.80	1.85	5.0	-0.05	0.06	22	0.03	4
72	4450	1.80	1.75	5.7	-0.04	0.09	25	0.09	5

Table 4. Determined abundances and isotopic ratios for programme stars

Element	NGC 4609 43	NGC 5316 31	NGC 5316 35	NGC 5316 45	NGC 5316 72	NGC 5316 Average*
[C/Fe]	-0.23 ± 0.01 (2)	-0.26 ± 0.02 (2)	-0.10 ± 0.02 (2)	-0.08 ± 0.03 (2)	-0.20 ± 0.04 (2)	-0.16 ± 0.07
[N/Fe]	0.63 ± 0.02 (6)	0.60 ± 0.05 (6)	0.82 ± 0.07 (6)	0.50 ± 0.05 (6)	0.72 ± 0.08 (6)	0.66 ± 0.12
[O/Fe]	0.11 (1)	-0.11 (1)	0.20 (1)	0.07 (1)	0.05 (1)	0.11 ± 0.11
C/N	0.55	0.54	0.48	1.05	0.48	0.64 ± 0.24
¹² C/ ¹³ C	23	22	23	24	24	23 ± 1
[Na/Fe] _{LTE}	0.42 ± 0.08 (4)	0.39 ± 0.06 (3)	0.35 ± 0.03 (3)	0.33 ± 0.08 (3)	0.45 ± 0.03 (3)	0.38 ± 0.05
[Na/Fe] _{NLTE}	0.33 ± 0.05 (3)	0.27 ± 0.06 (3)	0.26 ± 0.05 (2)	0.22 ± 0.07 (3)	0.33 ± 0.05 (3)	0.27 ± 0.04
[Mg/Fe]	-0.06 ± 0.01 (2)	-0.09 ± 0.05 (3)	-0.05 ± 0.06 (3)	-0.01 ± 0.11 (2)	0.04 ± 0.09 (3)	-0.03 ± 0.05
[Al/Fe]	0.15 ± 0.01 (2)	0.11 ± 0.08 (2)	0.16 ± 0.05 (2)	0.12 ± 0.01 (2)	0.12 ± 0.05 (2)	0.13 ± 0.02
[Si/Fe]	0.13 ± 0.07 (10)	0.06 ± 0.03 (8)	0.12 ± 0.04 (7)	0.13 ± 0.05 (7)	0.20 ± 0.02 (7)	0.13 ± 0.05
[Ca/Fe]	0.07 ± 0.08 (7)	0.01 ± 0.04 (3)	0.11 ± 0.05 (6)	0.10 ± 0.08 (5)	0.13 ± 0.02 (5)	0.09 ± 0.05
[Sc/Fe]	0.01 ± 0.04 (5)	0.07 ± 0.09 (3)	-0.05 ± 0.02 (3)	-0.05 ± 0.01 (3)	0.06 ± 0.03 (4)	0.01 ± 0.06
[Ti I/Fe]	0.02 ± 0.07 (17)	0.02 ± 0.07 (12)	-0.02 ± 0.03 (10)	0.06 ± 0.02 (12)	0.07 ± 0.06 (13)	0.03 ± 0.04
[Ti II/Fe]	0.02 ± 0.02 (2)	0.05 ± 0.02 (2)	0.03 ± 0.08 (2)	0.02 ± 0.03 (2)	0.04 ± 0.01 (2)	0.04 ± 0.01
[Cr/Fe]	0.06 ± 0.06 (10)	0.05 ± 0.06 (5)	-0.02 ± 0.03 (5)	0.04 ± 0.09 (6)	0.09 ± 0.07 (5)	0.04 ± 0.04
[Mn/Fe]	0.15 ± 0.06 (3)	0.12 ± 0.02 (4)	0.09 ± 0.01 (3)	0.25 ± 0.04 (3)	0.18 ± 0.09 (3)	0.16 ± 0.06
[Co/Fe]	0.13 ± 0.08 (4)	-0.02 ± 0.06 (6)	0.16 ± 0.06 (5)	0.26 ± 0.05 (5)	0.06 ± 0.09 (2)	0.12 ± 0.11
[Ni/Fe]	-0.02 ± 0.04 (15)	-0.03 ± 0.09 (14)	-0.05 ± 0.10 (10)	0.00 ± 0.10 (13)	0.07 ± 0.10 (18)	0.00 ± 0.05
[Y/Fe]	-0.01 ± 0.06 (5)	0.22 ± 0.12 (4)	0.15 ± 0.11 (4)	0.23 ± 0.09 (3)	0.12 ± 0.09 (3)	0.17 ± 0.05
[Zr/Fe]	0.04 ± 0.08 (2)	0.10 (1)	0.26 ± 0.06 (2)	0.27 ± 0.09 (2)	0.18 ± 0.09 (2)	0.24 ± 0.04
[Ba/Fe]	-0.09 ± 0.21 (2)	0.59 ± 0.06 (2)	0.30 ± 0.13 (2)	0.19 ± 0.13 (2)	0.22 ± 0.17 (2)	0.24 ± 0.05
[La/Fe]	0.05 ± 0.05 (3)	0.13 ± 0.05 (3)	0.32 ± 0.10 (3)	0.37 ± 0.06 (3)	0.29 ± 0.10 (3)	0.33 ± 0.03
[Ce/Fe]	0.03 ± 0.05 (3)	0.04 ± 0.11 (3)	0.23 ± 0.13 (4)	0.20 ± 0.09 (4)	0.14 ± 0.08 (4)	0.19 ± 0.04
[Pr/Fe]	0.07 ± 0.06 (2)	0.11 ± 0.04 (2)	0.30 ± 0.07 (2)	0.31 ± 0.06 (2)	0.28 ± 0.06 (2)	0.30 ± 0.01
[Nd/Fe]	0.10 ± 0.01 (4)	0.16 ± 0.08 (3)	0.31 ± 0.11 (3)	0.30 ± 0.06 (3)	0.34 ± 0.04 (3)	0.32 ± 0.02
[Eu/Fe]	-0.01 (1)	0.02 (1)	0.22 (1)	0.22 (1)	0.20 (1)	0.21 ± 0.01

* Star NGC 5316 31 was not included in the calculation of average abundance for neutron capture elements.

Abundances of chemical elements relative to iron $[\text{El}/\text{Fe}]^2$, a line-to-line scatter and a number of spectral lines used for the analysis are listed in Table 4. The ionisation stages of the investigated species can be found in Table 2. The abundance $[\text{Fe}/\text{H}]$ stands for both Fe I and Fe II abundances since they were required to be the same while determining a value of surface gravity in our method of analysis. For oxygen and europium just by one line were used for the analysis thus instead of line-to-line scatter we may consider the averaged random error which is about ± 0.06 dex (see Sect. 3). Table 4 also lists the determined C/N and

¹²C/¹³C ratios and averaged results for the open cluster NGC 5316.

4.2 Light elements

4.2.1 Sodium

Theoretical models which describe chemical mixing in evolved stars (Lagarde et al. 2012) predict an increase of sodium abundance depending on the turn-off mass. In the recent study by Smiljanic et al. (2016) it was shown that this is exactly the case. They plotted seven clusters with $[\text{Na}/\text{Fe}]$ determinations and made cautious conclusions about the increasing surface sodium abundances with increasing stellar mass. As we can see in Fig. 5, our clusters follow the theoretical models as well. Both LTE and NLTE values for the tar-

² We use the customary spectroscopic notation $[\text{X}/\text{Y}] \equiv \log_{10}(\text{N}_\text{X}/\text{N}_\text{Y})_{\text{star}} - \log_{10}(\text{N}_\text{X}/\text{N}_\text{Y})_{\odot}$.

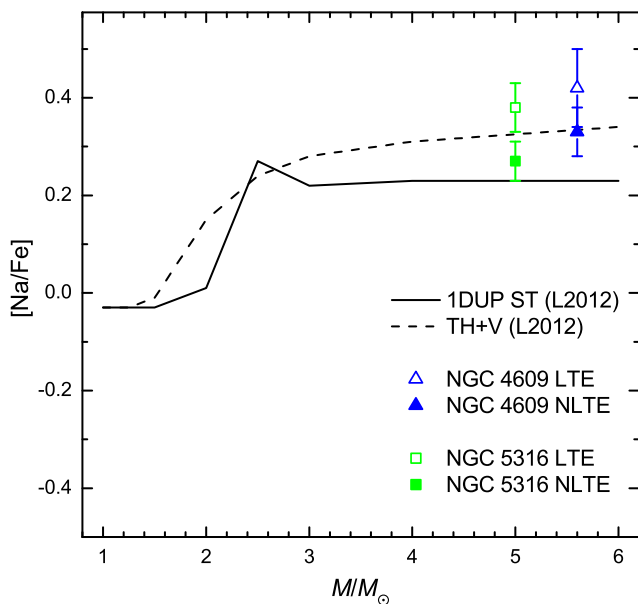


Figure 5. Mean $[\text{Na}/\text{Fe}]$ values in our sample clusters compared with theoretical extra-mixing models by Lagarde et al. (2012).

get clusters seem to indicate that the model which includes thermohaline- and rotation-induced mixing (Lagarde et al. 2012) agrees with the observed values well.

4.2.2 α -elements

In Fig. 6 we compare our two cluster results with theoretical models described by Magrini et al. (2009) and provided to us privately. All the abundance ratios in the model are normalized to the time and place of formation of the Sun. Further details can be found in the mentioned paper. Our results agree quite well with the $[\text{E}/\text{Fe}]$ models. The value for $[\text{O}/\text{H}]$ is somewhat higher for NGC 4609 and the value for $[\text{Mg}/\text{H}]$ is somewhat lower for NGC 5316, but these deviations are not significant (see e.g. Cunha et al. 2016 who presented results for 29 open clusters). When we calculate the average $[\alpha/\text{Fe}] = \frac{1}{4} ([\text{Mg}/\text{Fe}] + [\text{Si}/\text{Fe}] + [\text{Ca}/\text{Fe}] + [\text{Ti}/\text{Fe}])$ we get values of 0.04 dex for NGC 4609 and 0.06 dex for NGC 5316. These results are consistent with the thin disk α -element abundances.

4.3 Neutron-capture elements

The chemical composition of the three programme stars (35, 45, 72) in the cluster NGC 5316 is rather homogeneous. However, a noticeable difference is seen in the star NGC 5316 31 (see Table. 4). The main s-process element barium is significantly overabundant compared to the other stars and to other s-process element abundances in this star itself. We rule out errors in the atmospheric parameter determination for this star and a large sensitivity of Ba II lines to the microturbulent velocity being a cause of the unusual Ba abundance. The Ba II lines in this star are visually stronger in comparison to profiles of other s-process element lines which are also ionised.

Contrary to barium, other s- and r-process chemical elements (except yttrium), show a slight underabundance com-

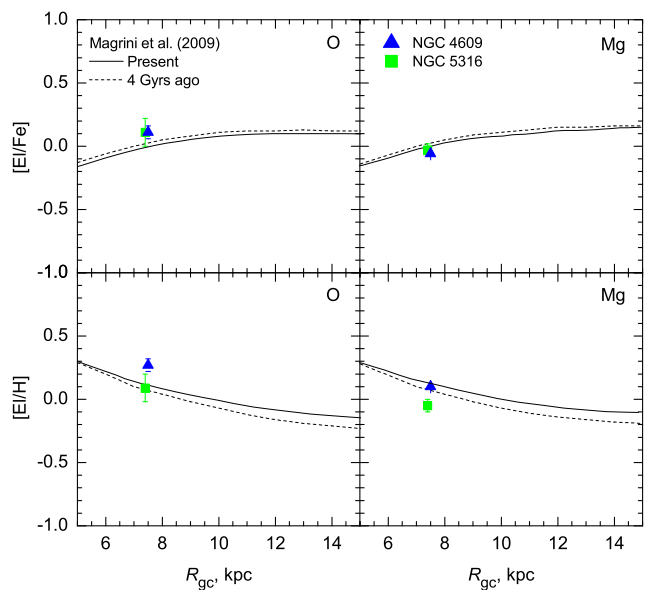


Figure 6. Oxygen and magnesium abundances compared to theoretical models by Magrini et al. (2009).

pared to other stars of this cluster. However, NGC 5316 31 does not fall into a category of barium-rich stars as defined by de Castro et al. (2016). Dias et al. (2001) give an 86% probability for this star being a member of NGC 5316. Its radial velocity determined in our work as well as in studies by Mermilliod et al. (2008), Frinchaboy & Majewski (2008) and others attribute the cluster membership for this star, thus we conclude that this star is an anomalous one. For these reasons we do not include the neutron-capture chemical elements of this star when calculating the average abundances of elements for the whole cluster as we conclude that this anomaly does not reflect the chemical composition of this cluster. Abundances of other chemical elements in this star agree well with those in other stars of this cluster.

For heavy chemical elements which are attributed to the s-process, we derived abundances of Y, Zr, Ba, La, Ce, and Nd. As described in Travaglio et al. (2004), 74% of yttrium and 67% of zirconium in the Sun are made by s-process reactions. For Ba, La, Ce, Nd, the s-process reactions contribute by 81%, 62%, 77%, 56%, respectively (Arlandini et al. 1999).

Fig. 7 shows the average abundances of neutron-capture chemical elements of our clusters as well as the average cluster results from other studies. We summarized the following previous studies: Maiorca et al. (2011); Jacobson & Friel (2013); Reddy et al. (2012, 2013, 2015); Mishenina et al. (2015); Mikolaitis et al. (2010, 2011a,b); Overbeek et al. (2016). We also show a thin disk chemical evolution model developed by Pagel & Tautvaisiene (1997). We do not display results of Eu obtained by Jacobson & Friel (2013) since they were redetermined by Overbeek et al. (2016) from the same spectra. The error-bars presented for every element are median errors computed from scatters around the mean values in all the studies used in plotting this figure.

NGC 5316 shows a good match with other studies and fails to concur the thin disk model. This result is the same as found in the majority of other studied open clusters and confirms the idea that s-process chemical elements in clus-

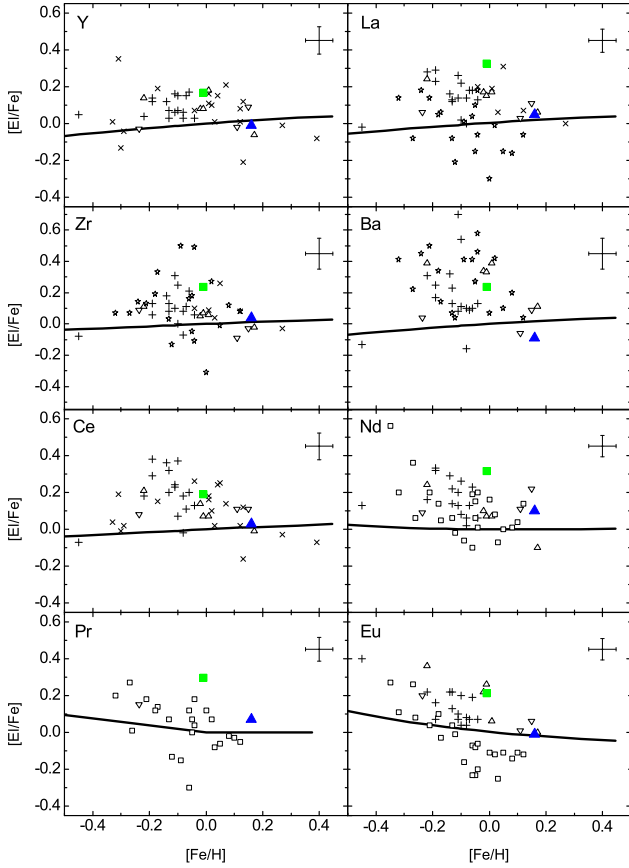


Figure 7. Neutron-capture element abundances of our target clusters compared to previous studies and the models for the thin disk stars by Pagel & Tautvaišienė (1997). Our clusters are indicated as filled symbols: a square for NGC 5316 and a triangle for NGC 4609. Plus signs indicate results by Reddy et al. (2012, 2013, 2015); triangles - results by Maiorca et al. (2011); stars - results by Jacobson & Friel (2013); open squares - Overbeek et al. (2016) and open reverse triangles indicate results by Mikolaitis et al. (2010, 2011a,b)

ters are higher than those in field stars (Marsakov et al. 2016 and references therein). As previously mentioned, the enrichment of AGB stars with s-process elements via the $(^{13}\text{C}(\alpha, n)^{16}\text{O})$ reaction is most visible in young open clusters (Maiorca et al. 2011; D’Orazi et al. 2009; Mishenina et al. 2015 etc.). This could explain the overabundance of these elements in NGC 5316, which is only 100 Myr old, compared to the thin disc.

The abundances of neutron-capture elements in NGC 4609 are lower by about 0.2 dex than in NGC 5316. Its abundances of s-process elements are almost the same as in the thin disk stars. This difference in abundances of two of our programme clusters is interesting, because both clusters are of a similar age, Galactocentric distance and even are at almost the same place in the Galaxy. However, one has to take into account, that NGC 4609 has only one identified red giant star, and that is the only star we have analysed in our work.

We determined abundances of praseodymium and europium which are attributed to the rapid neutron capture process (r-process) elements produced during supernovae ex-

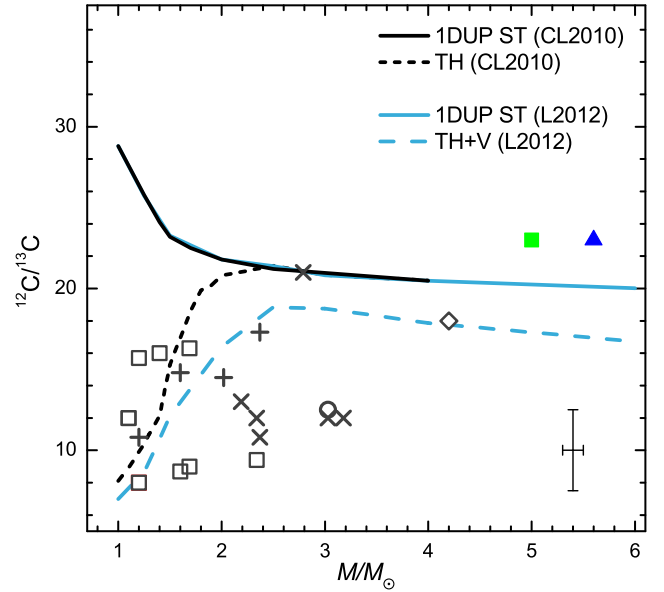


Figure 8. The average carbon isotope ratios in clump stars of open clusters as a function of stellar turn-off mass. Filled square indicates the value for NGC 5316, and filled triangle – for NGC 4609. Open squares indicate previous results by Tautvaišienė et al. (2000); Tautvaišienė et al. (2005); Mikolaitis et al. (2010, 2011a,b, 2012); Drazdauskas et al. (2016). Other symbols include results from Gilroy (1989) – pluses, Luck (1994) – open circles, Smiljanic et al. (2009) – crosses, Santrich et al. (2013) – open diamond. The solid lines (1DUP ST) represent the $^{12}\text{C}/^{13}\text{C}$ ratios predicted for stars at the first dredge-up with standard stellar evolutionary models of solar metallicity by Charbonnel & Lagarde (2010) (black solid line) and Lagarde et al. (2012) (blue solid line). The short-dashed line (TH) shows the prediction when just thermohaline extra-mixing is introduced (Charbonnel & Lagarde 2010), and the long-dashed line (TH+V) is for the model that includes both the thermohaline and rotation induced mixing (Lagarde et al. 2012). A typical error bar is indicated (Charbonnel & Lagarde 2010; Smiljanic et al. 2009; Gilroy 1989).

plosions. According to theoretical studies (Arlandini et al. 1999 and others) around 51% of praseodymium and 91% of europium are produced during such events. NGC 5316 has higher values of Pr and Eu compared to the thin disc. NGC 4609 agrees better with the thin disk models and shows solar ratios for r-process elements.

4.4 $^{12}\text{C}/^{13}\text{C}$ and C/N ratios

As already mentioned in the introduction of this paper, abundances of carbon and nitrogen together with C/N and especially $^{12}\text{C}/^{13}\text{C}$ ratios are important tools when trying to understand stellar evolution. All the accumulated chemical changes that happen in stars during the RGB phase are reflected in the atmospheres of He-core burning stars. Studying these changes can provide valuable insight into stellar evolution. Now it is clear, that the first dredge-up models alone cannot account for all the observed abundance changes. Eggleton et al. (2008) called this extra-mixing a $\delta\mu$ mixing, and concluded that it is a significant and inevitable process in low mass stars that are ascending the red giant branch for the first time. They could not accurately define

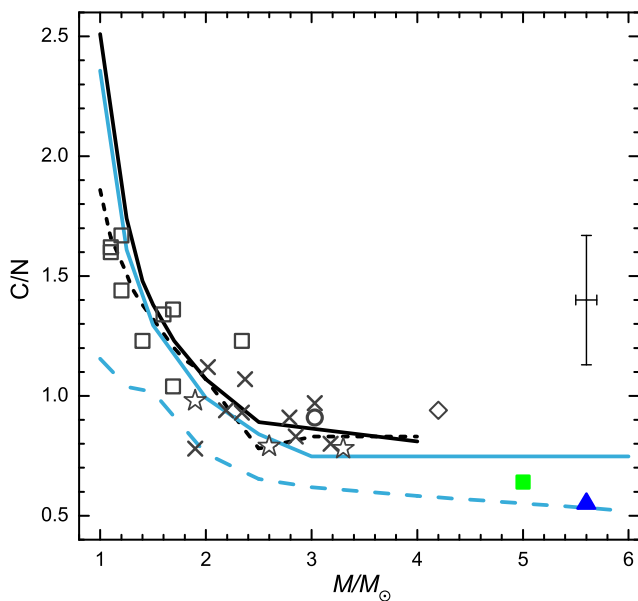


Figure 9. The average carbon-to-nitrogen ratios in clump stars of open clusters as a function of stellar turn-off mass. In addition to symbols in Fig. 8 here we include the results from Tautvaišienė et al. (2015) as open stars.

the speed of this mixing, but showed that it is relatively fast compared to the nuclear time scale. Their models, at the time, accounted well for the observed decrease in $^{12}\text{C}/^{13}\text{C}$ ratios than predicted before.

The recent models by Charbonnel & Lagarde and Lagarde et al. are based on the ideas of Eggleton et al. (2006), Ulrich (1972), Charbonnel & Zahn (2007), Kippenhahn et al. (1980). In their study Eggleton et al. found a mean molecular weight inversion (μ) in $1M_{\odot}$ stellar evolution model. It occurred right after the so-called luminosity bump on the RGB, when the H-burning shell encounters the chemically homogeneous part of the envelope. Ulrich (1972) predicted, that this μ -inversion is the outcome of the $^3\text{He}(^3\text{He}, 2p)^4\text{He}$ reaction. It does not occur earlier because the μ -inversion is low and negligible compared to a stabilising μ -stratification. Charbonnel & Zahn (2007) used the ideas by Ulrich (which were extended to non perfect gas by Kippenhahn et al. 1980), computed stellar evolution models introducing a double diffusive instability called thermohaline convection and showed its importance in the evolution of red giants. This mixing process connects the external wing of the hydrogen burning shell to the convective envelope and induces element abundance changes in the atmospheres of evolved stars.

Lagarde et al. (2012) further developed these models adding the effects of rotation-induced mixing. Typical initial zero-age main sequence rotation velocities were chosen which depend on stellar mass and are based on observed velocity distributions in young open clusters (Gaige 1993). In the models, the convective envelope rotates as a solid body, and the transport coefficients associated with the thermohaline- and rotation-induced mixing were simply added in the diffusion equation. The rotation-induced mixing modifies the internal chemical structure even before the RGB phase, but the results are only visible in later evolutionary stages.

Figs. 8–9 display the comparison between theoretical models and $^{12}\text{C}/^{13}\text{C}$ and C/N ratios of stars in different open clusters as a function of TO mass. The theoretical models include the first dredge-up, thermohaline (TH), and thermohaline and rotation (TH+V) induced mixing computed by Charbonnel & Lagarde (2010) and Lagarde et al. (2012). We included the observational results from other studies as well (Gilroy 1989; Luck 1994; Tautvaišienė et al. 2000; Tautvaišienė et al. 2005, 2015; Mikolaitis et al. 2010, 2011a,b, 2012; Smiljanic et al. 2009; Drazdauskas et al. 2016).

The turn-off masses for our clusters are 5.6 and $5 M_{\odot}$ for NGC 4609 and NGC 5316, respectively. All stars in our sample are considered as being the He-core burning stars. Compared with the theoretical models we can see that in this mass range extra-mixing does not have a significant effect and our mean $^{12}\text{C}/^{13}\text{C}$ values agree with the standard first dredge-up and thermohaline-induced mixing model (Charbonnel & Lagarde 2010) and are not lowered as much as predicted by the models where thermohaline- and rotation-induced mixing act together (Lagarde et al. 2012). The result of open cluster NGC 3114 by Santrich et al. (2013) lies below the first dredge-up model. Certainly, more clusters with large TO masses should be observed in order to have a clearer picture. The same is valid in case of C/N ratios (Fig. 9). C/N ratios have larger uncertainties, our results for both clusters are very close and seem to agree with both the first dredge-up and the thermohaline- and rotation-induced mixing models. The result of NGC 3114 this time is more close to the first dredge-up model.

This study further shows that we need more observational data to better understand the mixing processes in evolved stars and to make more precise models.

5 CONCLUSIONS

Two young open clusters were analysed for the first time using high resolution spectroscopy. The main atmospheric parameters and abundances of 23 chemical elements were determined. The main conclusions of our chemical composition analysis can be summarized as follows:

- (i) NGC 4609 has a slightly larger than solar metallicity of $[\text{Fe}/\text{H}] = 0.16 \pm 0.08$, a turn-off mass of about $5.6 M_{\odot}$ (with the age of 80 Myr), and a Galactocentric distance of about 7.5 kpc.
- (ii) NGC 5316 is of solar metallicity, its $[\text{Fe}/\text{H}] = -0.02 \pm 0.05$, the turn-off mass is about $5 M_{\odot}$ (with the age of 100 Myr).
- (iii) $^{12}\text{C}/^{13}\text{C}$ and C/N ratios and $[\text{Na}/\text{Fe}]$ agree quite well with the model which takes into account thermohaline- and rotation-induced mixing but within error limits also agree with the standard first dredge-up model.
- (iv) Comparison of oxygen, magnesium and other α -elements with theoretical models of Galactic chemical evolution revealed that both clusters follow the thin disk α -element trends.
- (v) The open cluster NGC 5316 confirms the enrichment s-process element abundances seen in other young open clusters compared to old clusters. The star NGC 5316 31 has an exceptionally high barium abundance. NGC 4609 has solar neutron-capture element-to-iron ratios.

There are few clusters of intermediate turn-off masses for which a detailed chemical composition is studied, therefore NGC 4609 and NGC 5316 add useful data to this small sample. Further spectroscopic analyses of other young clusters will be welcomed in order to investigate the abundance pattern in evolved intermediate mass stars.

ACKNOWLEDGEMENTS

This research has made use of the WEBDA database (operated at the Department of Theoretical Physics and Astrophysics of the Masaryk University, Brno), of SIMBAD (operated at CDS, Strasbourg), of VALD (Kupka et al. 2000), and of NASA's Astrophysics Data System. Bertrand Plez (University of Montpellier II) and Guillermo Gonzalez (Washington State University) were particularly generous in providing us with atomic data for CN and C₂ molecules, respectively. We thank Laura Magrini for sharing with us the Galactic chemical evolution models. AD, GT, YC, and VB were partly supported by the grant from the Research Council of Lithuania (MIP-082/2015). RS acknowledges support by the National Science Center of Poland through the grant 2012/07/B/ST9/04428.

REFERENCES

- Angelou G. C., Stancliffe R. J., Church R. P., Lattanzio J. C., Smith G. H., 2012, *ApJ*, **749**, 128
- Arlandini C., Käppeler F., Wisshak K., Gallino R., Lugaro M., Busso M., Straniero O., 1999, *ApJ*, **525**, 886
- Battinelli P., Capuzzo-Dolcetta R., 1991, *MNRAS*, **249**, 76
- Becker W., Fenkart R., 1971, *A&AS*, **4**, 241
- Bensby T., Feltzing S., Oey M. S., 2014, *A&A*, **562**, A71
- Biehl D., 1976, PhD thesis, PhD thesis, Univ. Kiel, (1976)
- Bressan A., Marigo P., Girardi L., Salasnich B., Dal Cero C., Rubele S., Nanni A., 2012, *MNRAS*, **427**, 127
- Burbidge E. M., Burbidge G. R., Fowler W. A., Hoyle F., 1957, *Reviews of Modern Physics*, **29**, 547
- Cantiello M., Langer N., 2010, *A&A*, **521**, A9
- Carraro G., Seleznev A. F., 2012, *MNRAS*, **419**, 3608
- Chanamé J., Pinsonneault M., Terndrup D. M., 2005, *ApJ*, **631**, 540
- Charbonnel C., 2006, in Montmerle T., Kahane C., eds, EAS Publications Series Vol. 19, EAS Publications Series. pp 125–146, doi:10.1051/eas:2006029
- Charbonnel C., Lagarde N., 2010, *A&A*, **522**, A10
- Charbonnel C., Zahn J.-P., 2007, *A&A*, **467**, L15
- Chen L., Hou J. L., Wang J. J., 2003, *AJ*, **125**, 1397
- Claria J. J., Lapasset E., 1989, *MNRAS*, **241**, 301
- Claria J. J., Lapasset E., Minniti D., 1989a, *A&AS*, **78**, 363
- Claria J. J., Lapasset E., Minniti D., 1989b, *A&AS*, **78**, 363
- Cunha K., et al., 2016, preprint, (arXiv:1601.03099)
- D'Orazi V., Magrini L., Randich S., Galli D., Busso M., Sestito P., 2009, *ApJ*, **693**, L31
- Denissenkov P. A., 2010, *ApJ*, **723**, 563
- Dias W. S., Lépine J. R. D., Alessi B. S., 2001, *A&A*, **376**, 441
- Dias W. S., Lépine J. R. D., Alessi B. S., 2002, *A&A*, **388**, 168
- Dias W. S., Monteiro H., Caetano T. C., Lépine J. R. D., Assafin M., Oliveira A. F., 2014, *A&A*, **564**, A79
- Drazdauskas A., Tautvaišienė G., Randich S., Bragaglia A., Mikolaitis Š., Janulis R., 2016, *A&A*, **589**, A50
- Eggleton P. P., Dearborn D. S. P., Lattanzio J. C., 2006, *Science*, **314**, 1580
- Eggleton P. P., Dearborn D. S. P., Lattanzio J. C., 2008, *ApJ*, **677**, 581
- Eichler D., Livio M., Piran T., Schramm D. N., 1989, *Nature*, **340**, 126
- Feinstein A., Marraco H. G., 1971, *PASP*, **83**, 218
- Freiburghaus C., Rosswog S., Thielemann F.-K., 1999, *ApJ*, **525**, L121
- Frinchaboy P. M., Majewski S. R., 2008, *AJ*, **136**, 118
- Gaige Y., 1993, *A&A*, **269**, 267
- Gilroy K. K., 1989, *ApJ*, **347**, 835
- Gonzalez G., Lambert D. L., Wallerstein G., Rao N. K., Smith V. V., McCarthy J. K., 1998, *ApJS*, **114**, 133
- Gratton R. G., Sneden C., Carretta E., Bragaglia A., 2000, *A&A*, **354**, 169
- Grevesse N., Sauval A. J., 2002, *Advances in Space Research*, **30**, 3
- Gurtovenko E. A., Kostyk R. I., 1989, Kiev Izdatel Naukova Dumka,
- Gustafsson B., Edvardsson B., Eriksson K., Jørgensen U. G., Nordlund Å., Plez B., 2008, *A&A*, **486**, 951
- Heiter U., et al., 2015, *Phys. Scr.*, **90**, 054010
- Iben Jr. I., 1965, *ApJ*, **142**, 1447
- Jacobson H. R., Friel E. D., 2013, *AJ*, **145**, 107
- Johansson S., Litzén U., Lundberg H., Zhang Z., 2003, *ApJ*, **584**, L107
- Jura M., 1987, *ApJ*, **313**, 743
- Kaufer A., Stahl O., Tubbesing S., Nørregaard P., Avila G., Francois P., Pasquini L., Pizzella A., 1999, *The Messenger*, **95**, 8
- Kharchenko N. V., Piskunov A. E., Röser S., Schilbach E., Scholz R.-D., 2005, *A&A*, **438**, 1163
- Kharchenko N. V., Piskunov A. E., Schilbach E., Röser S., Scholz R.-D., 2013, *A&A*, **558**, A53
- Kippenhahn R., Ruschenplatt G., Thomas H.-C., 1980, *A&A*, **91**, 175
- Kupka F. G., Ryabchikova T. A., Piskunov N. E., Stempels H. C., Weiss W. W., 2000, *Baltic Astronomy*, **9**, 590
- Lagarde N., Charbonnel C., Decressin T., Hagelberg J., 2011, *A&A*, **536**, A28
- Lagarde N., Decressin T., Charbonnel C., Eggenberger P., Ekström S., Palacios A., 2012, *A&A*, **543**, A108
- Lattanzio J. C., Siess L., Church R. P., Angelou G., Stancliffe R. J., Doherty C. L., Stephen T., Campbell S. W., 2015, *MNRAS*, **446**, 2673
- Lawler J. E., Wickliffe M. E., den Hartog E. A., Sneden C., 2001, *ApJ*, **563**, 1075
- Lind K., Asplund M., Barklem P. S., Belyaev A. K., 2011, *A&A*, **528**, A103
- Lindoff U., 1968, *Arkiv for Astronomi*, **5**, 1
- Luck R. E., 1994, *ApJS*, **91**, 309
- Magrini L., Sestito P., Randich S., Galli D., 2009, *A&A*, **494**, 95
- Maiorca E., Randich S., Busso M., Magrini L., Palmerini S., 2011, *ApJ*, **736**, 120
- Maiorca E., Magrini L., Busso M., Randich S., Palmerini S., Trippe O., 2012, *ApJ*, **747**, 53
- Marsakov V. A., Gozha M. L., Koval' V. V., Shpigel' L. V., 2016, *Astronomy Reports*, **60**, 61
- McWilliam A., 1998, *AJ*, **115**, 1640
- Mermilliod J. C., 1981, *A&AS*, **44**, 467
- Mermilliod J. C., Mayor M., Udry S., 2008, *A&A*, **485**, 303
- Mikolaitis Š., Tautvaišienė G., Gratton R., Bragaglia A., Carretta E., 2010, *MNRAS*, **407**, 1866
- Mikolaitis Š., Tautvaišienė G., Gratton R., Bragaglia A., Carretta E., 2011a, *MNRAS*, **413**, 2199
- Mikolaitis Š., Tautvaišienė G., Gratton R., Bragaglia A., Carretta E., 2011b, *MNRAS*, **416**, 1092
- Mikolaitis Š., Tautvaišienė G., Gratton R., Bragaglia A., Carretta E., 2012, *A&A*, **541**, A137
- Mishenina T., et al., 2015, *MNRAS*, **446**, 3651

- Neves V., Santos N. C., Sousa S. G., Correia A. C. M., Israelian G., 2009, *A&A*, **497**, 563
- Nishimura N., Takiwaki T., Thielemann F.-K., 2015, *ApJ*, **810**, 109
- Overbeek J. C., Friel E. D., Jacobson H. R., 2016, preprint, ([arXiv:1604.05735](https://arxiv.org/abs/1604.05735))
- Pagel B. E. J., Tautvaišienė G., 1997, *MNRAS*, **288**, 108
- Piatti A. E., Claria J. J., Abadi M. G., 1995, *AJ*, **110**, 2813
- Piskunov N. E., Kupka F., Ryabchikova T. A., Weiss W. W., Jeffery C. S., 1995, *A&AS*, **112**, 525
- Rahim M. A., 1966, *Astronomische Nachrichten*, **289**, 41
- Reddy A. B. S., Giridhar S., Lambert D. L., 2012, *MNRAS*, **419**, 1350
- Reddy A. B. S., Giridhar S., Lambert D. L., 2013, *MNRAS*, **431**, 3338
- Reddy A. B. S., Giridhar S., Lambert D. L., 2015, *MNRAS*, **450**, 4301
- Santrich O. J. K., Pereira C. B., Drake N. A., 2013, *A&A*, **554**, A2
- Smiljanic R., Gauderon R., North P., Barbuy B., Charbonnel C., Mowlavi N., 2009, *A&A*, **502**, 267
- Smiljanic R., et al., 2016, *A&A*, **589**, A115
- Snedden C., Lawler J. E., Cowan J. J., Ivans I. I., Den Hartog E. A., 2009, *ApJS*, **182**, 80
- Stetson P. B., Pancino E., 2008, *PASP*, **120**, 1332
- Strobel A., 1991, *A&A*, **247**, 35
- Tautvaišienė G., Edvardsson B., Tuominen I., Ilyin I., 2000, *A&A*, **360**, 499
- Tautvaišienė G., Edvardsson B., Puzeras E., Ilyin I., 2005, *A&A*, **431**, 933
- Tautvaišienė G., Edvardsson B., Puzeras E., Barisevičius G., Ilyin I., 2010, *MNRAS*, **409**, 1213
- Tautvaišienė G., et al., 2015, *A&A*, **573**, A55
- Travaglio C., Gallino R., Arnone E., Cowan J., Jordan F., Sneden C., 2004, *ApJ*, **601**, 864
- Twarog B. A., Ashman K. M., Anthony-Twarog B. J., 1997, *AJ*, **114**, 2556
- Ulrich R. K., 1972, *ApJ*, **172**, 165
- Wachlin F. C., Miller Bertolami M. M., Althaus L. G., 2011, *A&A*, **533**, A139
- Woosley S. E., Wilson J. R., Mathews G. J., Hoffman R. D., Meyer B. S., 1994, *ApJ*, **433**, 229
- Zhu Z., Shen M., 2013, in de Grijs R., ed., *IAU Symposium Vol. 289, Advancing the Physics of Cosmic Distances*. pp 444–447, [doi:10.1017/S1743921312021928](https://doi.org/10.1017/S1743921312021928)
- de Castro D. B., Pereira C. B., Roig F., Jilinski E., Drake N. A., Chavero C., Silva J. V. S., 2016, *MNRAS*,
- Škoda P., Draper P. W., Neves M. C., Andrešič D., Jenness T., 2014, *Astronomy and Computing*, **7**, 108